

State-resolved collisional energy transfer in highly excited NO 2 . II. Vibrational energy transfer in the presence of strong chemical interaction

Bernd Abel, Norbert Lange, Florian Reiche, and Jürgen Troe

Citation: *The Journal of Chemical Physics* **110**, 1404 (1999); doi: 10.1063/1.478015

View online: <http://dx.doi.org/10.1063/1.478015>

View Table of Contents: <http://scitation.aip.org/content/aip/journal/jcp/110/3?ver=pdfcov>

Published by the [AIP Publishing](#)

Articles you may be interested in

Rotationally specific rates of vibration–vibration energy exchange in collisions of NO ($X^2\Pi_{1/2}, v=3$) with NO ($X^2\Pi, v=0$)

J. Chem. Phys. **111**, 9296 (1999); 10.1063/1.479843

State-resolved collisional quenching of highly vibrationally excited pyridine by water: The role of strong electrostatic attraction in $V \rightarrow RT$ energy transfer

J. Chem. Phys. **111**, 3517 (1999); 10.1063/1.479635

State-resolved collisional energy transfer in highly excited NO 2 . I. Cross sections and propensities for J, K, and m J changing collisions

J. Chem. Phys. **110**, 1389 (1999); 10.1063/1.478014

A combined experimental and theoretical study of rotational energy transfer in collisions between NO ($X^2\Pi_{1/2}, v=3, J$) and He, Ar and N 2 at temperatures down to 7 K

J. Chem. Phys. **109**, 3882 (1998); 10.1063/1.476517

State-resolved collisional relaxation of highly vibrationally excited pyridine by CO 2 : Influence of a permanent dipole moment

J. Chem. Phys. **108**, 6185 (1998); 10.1063/1.476061



State-resolved collisional energy transfer in highly excited NO₂. II. Vibrational energy transfer in the presence of strong chemical interaction

Bernd Abel,^{a)} Norbert Lange,^{b)} Florian Reiche, and Jürgen Troe
*Institut für Physikalische Chemie der Universität Göttingen, Tammannstrasse 6,
37077 Göttingen, Germany*

(Received 14 May 1998; accepted 5 October 1998)

The state-resolved collisional self-relaxation of highly (optically) excited NO₂ ($E_{\text{int}} \approx 18\,000\text{ cm}^{-1}$) in a thermal cell has been probed directly using time-resolved optical double resonance spectroscopy. The thermally averaged state-to-state cross sections have been derived from a master equation analysis of the kinetic traces. Rovibrational energy transfer (intramolecular $V-V, V-T, R$) was found to be more than an order of magnitude less efficient than pure rotational energy transfer ($R-T, R-RT$) within a vibrational state. The obtained cross sections for vibrational energy transfer are discussed with respect to the different relaxation mechanisms of the molecule, i.e., direct “fast” relaxation $\text{NO}_2(\nu_i) + \text{NO}_2 \rightarrow \text{NO}_2(\nu_f) + \text{NO}_2$ and complex forming collisions $\text{NO}_2(\nu_i) + \text{NO}_2 \rightarrow \text{N}_2\text{O}_4 \rightarrow \text{NO}_2(\nu_f) + \text{NO}_2$, and compared with high pressure recombination rates k_∞ . The experiments show that the observed collisions are closer to the impulsive than to the complex forming limit. In addition, we have discussed the magnitude of the experimental relaxation rates in terms of excited state couplings and the influence of vibronic chaos on the relaxation of highly excited NO₂. © 1999 American Institute of Physics. [S0021-9606(99)00402-X]

I. INTRODUCTION

This paper is concerned with details of state-to-state vibrational and rotational energy transfer within the excited state manifold of a small polyatomic molecules, namely NO₂, induced by gas phase collisions. Since in many kinetic systems collisional energy transfer competes with reactive processes, the mechanisms of collisional energy transfer of small molecules at high levels of vibrational excitation are of fundamental interest for uni- and bimolecular dynamics.¹ The understanding of collisional energy transfer at chemically significant energies, however, is still a challenge for experimental^{2–6} and theoretical investigations.^{7–13} Over the past decade there has been much experimental progress in understanding collisional energy relaxation for small and even for large molecules. Transient ultraviolet (UV) absorption,¹⁴ infrared (IR) emission,¹ Fourier transform IR emission spectroscopy,¹⁵ kinetically controlled selective ionization,¹⁶ resonance enhanced multiphoton excitation,¹⁷ time-resolved diode laser spectroscopy of bath molecules,^{4–6} and photothermal techniques¹⁸ implemented in time and energy-resolved pump/probe experiments have all been successfully used to monitor the energized species or their collision partners and to extract quantities such as the average energy transferred in a collision $\langle E \rangle$ and (in some cases) the second moment of energy transfer $\langle E^2 \rangle$ over a wide energy range as a function of the complexity of the parent molecule and the nature of the collision partner. Recently, Hippler and Troe,¹ and Flynn and Weston⁴ reviewed the state-of-the-art experiments in this field. In order to study collisional energy

transfer mechanisms directly, the role of intramolecular couplings and dynamics on intermolecular energy transfer, as well as the role of state and rotation specific dynamics at high (chemically significant) internal energies, experiments that are able to follow these processes at a quantum state-resolved level of detail on a (near) single collision time scale are highly desirable.⁶ New experimental methods such as pulsed molecular beams, dispersed laser fluorescence, and double resonance techniques are now providing exciting new results about state-resolved vibrational and rotational energy transfer at high and low collision energies and low to intermediate excitation energies. The question remains open and questionable whether these results can be simply extrapolated towards high internal energies. In spite of the fundamental interest in the state-resolved energy transfer of (small) molecules at high internal energies, only a very limited number of direct, state-resolved experimental data on the relaxation of polyatomic molecules at high vibrational energy exists. Due to experimental progress in the state-selective preparation and detection of highly excited molecules, laser based double resonance type experiments on C₂H₂,^{19,20} HCN,²¹ H₂CO,^{22,23} and NO₂²⁴ have been possible. In these experiments, energy and population redistribution were directly monitored within the highly excited polyatomic molecules and they provided a first glimpse of state-resolved collisional energy transfer at energies above $10\,000\text{ cm}^{-1}$. In contrast, at low internal energies, detailed studies are much more common, leading to a (near) consistent physical picture of inelastic processes in this regime.^{5,25–27} These advances in experimental techniques, together with the availability of enhanced computing power, have done much to inspire new theoretical and computational developments. It has now been possible to do accurate quantum mechanical scattering cal-

^{a)}Electronic mail: BABEL@gwdg.de

^{b)}Present address: DGR-LPAS, Ecole Polytechnique Federale de Lausanne, 1015 Lausanne, Switzerland.

culations on the vibrational and rotational excitation of diatomic and triatomic molecules in collisions with atoms for relatively low collision energies.⁹ Furthermore, slightly more approximate quantum scattering calculations can be done on polyatomic molecules and on collisions between molecules. Also, the methods of *ab initio* quantum chemistry are now providing the first potential energy surfaces that are needed for molecular collision calculations of good quality. The closed-coupled infinite-order-sudden approximation (CC-IOSA) approach of Clary⁹ seems to be a powerful approach that enables calculations of state resolved energy transfer between polyatomic molecules to be carried out. In the case of complex forming collisions the approach of Takayanagi,²⁸ Sakimoto,²⁹ and Dashevskaya *et al.*³⁰ is very promising. The latter studied nonadiabatic effects within the framework of the statistical adiabatic channel model (SACM). Unfortunately, all these highly sophisticated approaches could only be applied to very simple systems or colliding species with rather low internal energies. For highly excited molecules there is no explicit general theory available or applicable. Low dimensional “theoretical models” for $V-T$ and $V-V$ energy transfer based upon the classical Landau–Teller (LT), and the Schwartz–Slawsky–Herzfeld theory³¹ (SSH) have been modified by Tanczos³² and Stretton³³ and later by Parmenter and Tang^{34,35} to describe the vibrational energy transfer of moderately excited polyatomic species as well as their energy dependence. It is not yet clear whether these models can be extended to higher energy regions. This makes the interpretation of state-resolved experiments at chemically interesting internal energies quite difficult. Due to the large uncertainties of calculated cross sections of molecule+molecule (atom) collisions, especially those involving polyatomic molecules like NO_2 – NO_2 collisions, in practice, it is usually necessary to rely on high-quality experimental data for guidance, and to resort to one or more well-established approximate (but computationally tractable) dynamic theories to interpret and rationalize such data.

NO_2 has been the subject of innumerable studies, partly because it is one of the few chemically stable radicals, and partly because of its strong and complex absorption in the visible.^{36,37} Despite the large number of studies involving the NO_2 molecule the understanding of collisional energy transfer in this system is far from being complete. Recent experimental attempts to investigate the kinetics of NO_2 relaxation have relied mainly on the observation of excited NO_2 emission and chemiluminescence.^{38,39(a)(b)} In addition, the competition between unimolecular reaction and energy transfer has been measured in a series of early Stern–Volmer experiments.⁴⁰ In recent energy transfer studies Dai *et al.*,¹⁵ Barker *et al.*,¹⁸ Sander *et al.*,⁴¹ and Flynn *et al.*^{6,42} used single photon excitation, and followed the time evolution of the system by infrared and visible emission, optothermal detection, or by monitoring quantum states of the small bath gas molecules. Just at the dissociation threshold Reisler *et al.*⁴³ measured activating collisions of NO_2 in crossed molecular beams by recording NO photofragment spectra. These experiments provided quite detailed information about vibrational relaxation processes and a first clear picture about the energy dependence of $\langle \Delta E \rangle$, overall relaxation rates,

mechanisms, and energy deposition in bath molecules. However, in almost all experiments, individual rovibrational states of the parent molecules could neither be resolved nor studied.

The self-relaxation of the free radical NO_2 is particularly interesting at high internal energies because highly excited NO_2 may serve as an ideal model system to study state-resolved vibrational energy transfer of small molecules in competition to bimolecular (or unimolecular) reaction. This opportunity comes from the fact that NO_2 molecules recombine to form N_2O_4 in a mildly exothermic bimolecular reaction.⁴⁴

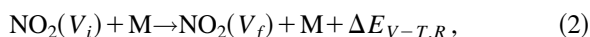


$$\Delta_r H_{298}^0 = -53 \text{ kJ mol}^{-1} \text{ (4430 cm}^{-1}\text{)}. \quad (1)$$

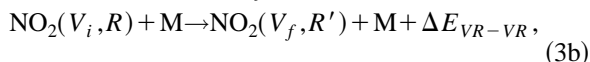
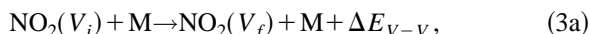
This recombination also provides one of the rare opportunities for studying the influence of strong attractive chemical forces on vibrational relaxation rates in collisions between neutral species. Due to the strong excited state mixing of highly excited NO_2 (${}^2B_2/{}^2A_1$ mixing, and conical intersection) the study of the influence of strong excited state mixing on the rotational and vibrational energy transfer in self-collisions is possible.

In order to clarify terms and make possible processes more transparent, let us assume that NO_2 molecules are excited optically to a vibrational state which can be specified by a set of vibrational quantum numbers, abbreviated as V , and then interact with an unexcited NO_2 molecule (M). In this case several possible energy transfer processes can be expected:

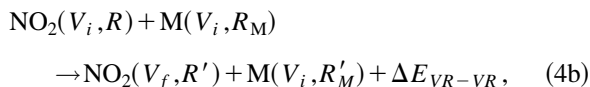
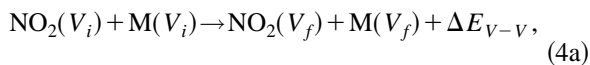
- (i) vibrational-to-translational/rotational ($V-T,R$) transfer



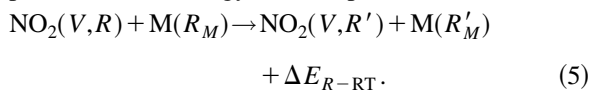
- (ii) vibration-to-vibration ($V-V$) transfer (intramolecular)



- (iii) vibration-to-vibration ($V-V$) transfer (intermolecular)



- (iv) pure rotational energy transfer processes (RET)



The latter process is pure rotational energy transfer accompanying, and competing with rovibrational energy transfer. Being about 1–2 orders of magnitude faster than vibrational energy transfer, rotational energy transfer tends to equilibrate a rotational manifold within a vibrational state

and usually makes rovibrational state-to-state cross sections for vibrational energy transfer difficult to extract from time and state-resolved measurements.

The principal relaxation pathways, Eqs. (2)–(5) discussed above only describe the net outcome of a collision. However, these pathways may belong to very different relaxation mechanisms with regard to the collision time and dynamics. We would like to point out that we distinguish here impulsive collisions (governed by the kinematics of the collision) and collisions which form long lived complexes, exchange energy, and which may be regarded to be almost recombinations of two particles forming an activated molecule which in turn redissociates. With regard to the molecular dynamics in collisions, complex forming and direct (impulsive) collisions can be regarded as limiting cases and the actual collision dynamics is expected to be somewhere in between.

The double resonance approach used here employs one laser pulse to prepare an initial rovibrational population, and a second to probe the subsequent growth and decay of population, either in the initially prepared state or other states populated by the specific energy transfer processes, offering the opportunity to perform measurements of rotationally resolved $V-V$ transfer. The combination of time-resolved double resonance spectroscopy and master equation modeling of the data provided state-to-state rovibrational energy transfer rate constants (average cross sections) in NO_2 – NO_2 collisions. In part I of this series,^{45(a)} we investigated the rotational energy transfer cross sections and the propensities for J , K , and m_J changing collisions. In the present paper, we will focus on the vibrational energy transfer in collisions in the presence of strong intramolecular coupling and strong intermolecular chemical interaction. The competition between inelastic and truly reactive collisions of NO_2 with other (reactive) collision partners will be published in part III of this series.

II. EXPERIMENTAL TECHNIQUE

Our sequential time-resolved optical double resonance technique is depicted in Fig. 1 and has been described in detail in part I of this series and in Ref. 24, so that only a brief summary will be given here. According to Fig. 1, we used the output of a Lambda Physik Scanmate 2000E dye laser pumped by the second harmonic of a Continuum NY81C-10 Nd:YAG laser (10–20 mJ, bandwidth: $0.3\text{--}0.03\text{ cm}^{-1}$; pulse duration: 10 ns) and a Lambda Physik EMG 101 XeCl excimer laser pumped Lambda Physik LPD 3000 dye laser [pulse energy: 10–15 mJ, bandwidth: $0.3\text{--}0.04\text{ cm}^{-1}$ (étalon); pulse width: 15–20 ns] in our sequential optical double resonance technique for spectral assignment, the preparation, and the time-resolved probe of the populated states. Double resonance signals were monitored *via* an observation of the UV fluorescence from the final state (2^2B_2) to the ground state (X^2A_1). The two counterpropagating slightly collimated ($f=1.5\text{ m}$) and parallel polarized laser beams were overlapped in a stainless-steel cell containing the thermal NO_2 sample (150–700 μbar), and the fluorescence was collected with a $f/1.2$ optics and monitored by a Thorn EMI 9635 QB photomultiplier. A Burleigh Instruments WA

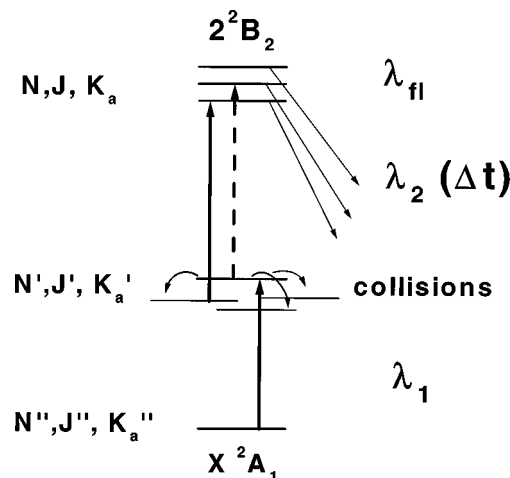


FIG. 1. Experimental pump and probe scheme.

5500 wavemeter was used for wavelength calibration and NO_2 pressures were measured by a capacitance baratron. NO_2 was obtained from Messer–Griesheim and used without further purification.

III. SPECTROSCOPY OF SELECTED STATES

State-resolved experimental investigations of collisional energy transfer require spectroscopically well characterized eigenstates. The relevant eigenstates for rovibrational energy transfer relevant to this investigation are summarized in Table I. These states, which are a small subset of all eigenstates in this particular energy range, have been assigned by a sequential double resonance technique, as described in part I of this series and Refs. 24 and 45. All states have been found to be strongly perturbed and mixed, however even in this case where vibronic chaos is established among the vibrational levels of highly excited states, the eigenstates could be unambiguously assigned. The fluorescence lifetimes of the considered eigenstates is larger than $\tau_{fl} > 5\text{ }\mu\text{s}$, such that the collisionally induced processes considered here were undisturbed. This has been verified by measuring total depopulation rates as a function of pressure. NO_2 is a stable radical with total angular momentum $J = N \pm S$ being a half integral. As was done in part I, the NO_2 molecule was treated as a spin-less particle with an angular momentum quantum number N . N is, of course, in this case not a rigorously conserved quantum number but we found out that it is sufficient to consider the change of N and K in the rotational energy transfer of the molecule. Note, an angular momentum change of “ $\Delta J = n$ ” throughout this paper means that N changed by n . For other peculiarities of the spectroscopy of these states and the ground and 2^2B_2 state, we refer to Refs. 24 and 45–47.

The different vibrational states and their origins could be distinguished in the experiment by plotting the spectroscopically determined term energies against $N(N+1)$, however, the vibrational “assignment” of the states was not possible in this energy region due to vibronic chaos.^{37,48,49} As shown in Table I the eigenstates in this energy transfer study belong to two energetically very close vibronic bands^{24,45,50} with

TABLE I. OODR transitions^a and assignments in the 563–566 nm range.

$N(\nu_{\text{pump}})$	$K_a(\nu_{\text{pump}})$	Vib. No. ^b	Energy/cm ⁻¹	Pump trans.	$\nu_{\text{pump}}/\text{cm}^{-1}$	Probe trans.	$\nu_{\text{probe}}/\text{cm}^{-1}$	Label/ Ref.
3	0	1	17 716.33	(3,0)' ← (4,0)''	17 707.92	(5,1) ← (''4,0'')'	22 431.43	30(1) ^c
5	0	1	17 724.33	(5,0)' ← (6,0)''	17 706.60	(7,1) ← (''6,0'')'	22 434.04	50(1) ^c
7	0	1	17 736.08	(7,0)' ← (8,0)''	17 705.66	(9,1) ← (''8,0'')'	22 435.71	70(1) ^c
9	0	1	17 750.07	(9,0)' ← (10,0)''	17 703.83	(11,1) ← (''10,0'')'	22 437.92	90(1) ^c
8	1	1	17 751.06	(8,1)' ← (7,1)''	17 719.75	(10,2) ← (''9,1'')'	22 431.13	81(1) ^c
3	0	2	17 717.85	(3,0)' ← (4,0)''	17 709.39	(5,1) ← (''4,0'')'	22 430.12	30(2) ^d
5	0	2	17 726.45	(5,0)' ← (6,0)''	17 718.00	(7,1) ← (''6,0'')'	22 431.83	50(2) ^c
7	0	2	17 737.82	(7,0)' ← (8,0)''	17 720.13	(8,1) ← (''8,0'')'	22 425.44	70(2) ^c
9	0	3	17 794.77	(9,0)' ← (8,0)''	17 764.46	(9,1) ← (''10,0'')'	22 405.85	90(3) ^d
7	0	3a	17 780.30	(7,0)' ← (6,0)''	17 762.55	(9,1) ← (''8,0'')'	22 400.76	70(3a) ^d
13	0	1	17 773.06	(13,0)' ← (12,0)''	17 707.27	(11,1) ← (''12,0'')'	22 408.4	130(1) ^c
6	1	1	17 737.92	(6,1)' ← (5,1)''	17 717.85	(6,2) ← (''7,1'')'	22 419.2	61(1) ^c
11	1	1	17 777.20	(11,1)' ← (10,1)''	17 722.56	(11,0) ← (''12,1'')'	22 399.2	111(1) ^c

^aIn general there are two transitions for the pump and 3–6 transitions (depending on K_a) for the probe laser (see double resonance spectra). We list here only the transitions which have been used in the energy transfer experiments and which are free from spectral overlap with other transitions. The wavelength calibration is accurate within 0.01–0.02 cm⁻¹. The primes ', ' , and no prime denotes the ground state, intermediate state, and final excited state, respectively.

^bAlthough the vibrational quantum numbers cannot be assigned in this energy region the rotational levels belonging to the same vibration can be found by plotting the term energies of the states vs $J(J+1)$. J is in this case N (the rotational angular momentum without spin) and the spin S is not considered here.

^cShibuya *et al.*, J. Phys. Chem. **97**, 8889 (1993).

^dThis work.

origins at 17 711.33 and 17 712.59 cm⁻¹ and one band at 17 754.89 cm⁻¹. Measurements of the population of intermediate states were carried out by tuning the two lasers to the corresponding pump and probe transitions and changing the time delay between the pulses.

IV. SCALING OF STATE-RESOLVED VIBRATIONAL ENERGY TRANSFER (VET) CROSS SECTIONS AND RATES

The many individual quantum state-resolved rate constants connecting individual rovibrational levels are not completely independent quantities. In particular, the rates for processes which differ only slightly in initial and/or final states are strongly correlated, and their correlations may, in principle, be derived *ab initio* from scattering theory. While those calculations are more or less straightforward, they can at the same time also be very complex and time consuming, especially for highly excited species. In any case a good intermolecular potential energy surface is required for these calculations which are by no means well known or easily determined, especially if one of the collision partners is highly excited or in an excited electronic state, as it is the case for NO₂.

Scattering theory should in principle be able to calculate state-resolved cross sections for vibrational and rotational relaxation of small molecules for various collision energies e.g., in the limits of impulsive and complex forming collisions and in situations in between. However, in a few cases it has now been possible to do accurate quantum mechanical scattering calculations on the vibrational and rotational excitation of diatomic and triatomic molecules in collisions with atoms for relatively low collision energies.⁹ In the limit of complex forming collisions at low collision energies⁸ the statistical approach within the framework of the SACM³⁰ may

be promising. In this case energy transfer probabilities are investigated mapping out all possible nonadiabatic transitions.

Unfortunately all these highly sophisticated approaches could only be applied to very simple systems or colliding species of rather low internal energies. In either case general scaling prescriptions for the extractions of state-resolved energy transfer cross sections are difficult to obtain. In practice, it is therefore necessary to start from high-quality experimental data and use them for guidance, and to use well-established approximate scaling expressions derived from IOS scattering theory or from Landau–Teller, SSH theory,³¹ or perturbation theory to extract and interpret the detailed state-resolved data.

In our data evaluation we have assumed that the collisions we observe, i.e., collisions at high energies above E_0 of N₂O₄, are closer to the impulsive (sudden) limit than to the complex-forming (statistical) limit. In the discussion we will discuss and justify this point of view and provide firm evidence for this approach.

Therefore, we used a classical energy gap scaling law for the states-resolved energy transfer rates. Scaling relations based solely on the magnitude of the energy defect in a rovibrational energy exchange have been successful in a variety of systems. This energy gap scaling has its origins in the classical Landau–Teller model where³¹

$$P \propto \exp[-\pi^2 \Delta E^2 / (2 \alpha^2 h^2 k T)]^{1/2} \quad (6)$$

(with α being the reciprocal of a length, the measure of the “hardness” of the molecule on impact).

In the original and modified SSH models⁵¹ we can write

$$P_{if} = P_0 g_f \cdot |U_{if}|^2 \cdot I(\Delta E_{if}, \mu, T, L, \epsilon) \quad (7)$$

(where P_0 is a steric factor, μ is the reduced mass, ϵ is the

Lennard-Jones well depth, g_f is the degeneracy of the final state, L is the repulsive exponential–potential range parameter, and T is the temperature).

The integral I has its main dependence from the energy gap ΔE , i.e., is a steeply decreasing function of the energy gap, and is well approximated by an exponential attenuation term. An exponential term is also used in the modified SSH model of Parmenter and Tang (SSH-PT).³⁴

We have found that the overall probability for rovibrational energy transfer in collisions between rovibrational states in NO_2 is well described by an energy gap law taking into account the degeneracy of the final state, as shown in Eq. (7).

V. KINETIC MODEL

In order to extract the thermally averaged state-to-state rate constants or cross sections for (ro)vibrational energy transfer we modeled the population transfer among a specified set of vibrational states with considerable rotational substructure employing a standard discrete master equation approach. This approach was necessary because these types of experiments still sum (and average) over all possible pathways between the initial and the final states, although initial and final states are completely resolved. This makes the extraction of state-to-state cross sections still a nontrivial problem. If \mathbf{N} is the array of state populations and \mathbf{K} is the matrix of the rate constants connecting these states, the time evolution of \mathbf{N} is given by:

$$\dot{\mathbf{N}} = \mathbf{K}\mathbf{N}. \quad (8)$$

The time-dependent array of populations $\mathbf{N}(t)$ can be obtained either by calculating the eigenvalues of \mathbf{K} or by integrating the set of coupled differential equations. We integrated the coupled differential system by a numerical Runge–Kutta method with adaptive step size. The set of discrete differential equations that has to be integrated can be written as:

$$\frac{dN_i}{dt} = \sum_{j \neq i} k_{ij}N_j + k_{ii}N_i = \sum_j k_{ij}N_j, \quad (9)$$

where k_{ij} is the rate constant of energy transfer from state j to state i and k_{ii} is the total depopulation rate of state i . The total depopulation rates are related to the rate constants of energy transfer by the conservation criterion:

$$k_{ii} = - \sum_{j \neq i} k_{ij}. \quad (10)$$

To account for the time dependent population of the pumped level by the pump source a term was added to the corresponding equation:

$$\frac{dN_p}{dt} = \sum_j k_{pj}N_j + \alpha I(t), \quad (11)$$

where $I(t)$ is the experimental pulse profile of the pump laser and α is a phenomenological proportionality coefficient of the population “source term.”

For modeling the “intravibrational” parts of the energy transfer problem, i.e., the rotational energy transfer in colli-

Model RET

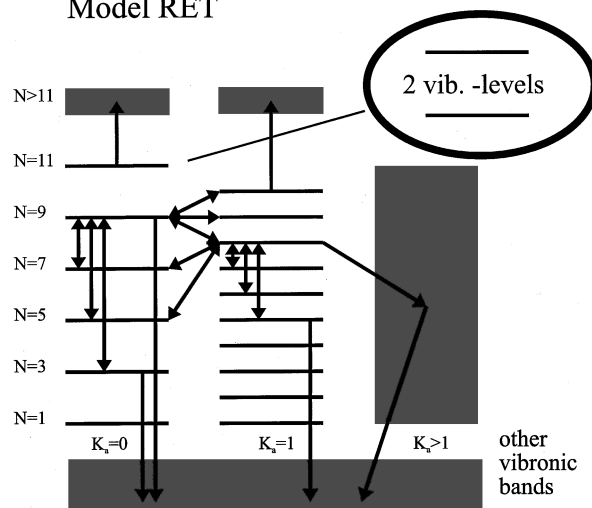


FIG. 2. Kinetic model for rotational energy transfer within a rotational manifold of a vibrational state.

sions within a rotational manifold of a vibrational state, we used the modified RET model depicted in Fig. 2 and all the energy transfer parameter of part I. In this case the simplified model consisted of collisionally coupled states with $N = 1 - 13/K_a = 0$ and $N = 1 - 12/K_a = 1$, all other states with $N > 13/12$ or $K_a > 1$ were represented by baths of states which were not allowed to feed back into the system of single states. The two vibrational levels in the final state region were explicitly taken into account. The $2J+1$ rotational m_J sublevels of each individual rotational level could not be taken into account explicitly. In order to model vibrational energy transfer between initial and final rovibronic states we included the relevant number and energetic positions of vibrational states in the model. Unfortunately, a fundamental problem and a small uncertainty in modeling the vibrational energy transfer turned out to be the unknown number and positions of the vibronic bands in the investigated energy region. We included all known vibronic levels from Jost *et al.*⁵⁰ such that we ended up taking three vibrational states which were either pumped or probed and four more vibronic bands which were not probed explicitly into account, each of them with the rotational substructure (levels and baths) shown in Fig. 3. We carefully checked the possible errors by including or excluding one more or one less vibrational level in the simulation, a modification that caused variations in the state specific rate constants by not more than 20%–30%. In addition, we measured collisionally induced double resonance spectra under nearly single collision conditions which gave identical results [but less signal to noise (S/N)] within the experimental error. The number of missing levels and the approximate number of levels in this energy region can be further checked by evaluation of the vibrational density of states in this range.

In the system of N states there are $N(N-1)$ different rate constants connecting these states. Therefore it is impossible to vary each rate constant individually. We decided to scale the rotational energy transfer within a vibrational state, as in part I, by an angular momentum based scaling law

$$k_{if}^{\text{ECS-EP}} = (2J_f + 1) \exp\left(\frac{E_{j_i} - E_{j_f}}{kT}\right) \times \sum_{\Lambda} \begin{pmatrix} j_i & j_f & \Lambda \\ 0 & 0 & 0 \end{pmatrix}^2 \cdot (2\Lambda + 1) \cdot F_K F_J k_{\Lambda \rightarrow 0}$$

with

$$k_{\Lambda \rightarrow 0} = A(T) \cdot [\Lambda(\Lambda + 1)]^{-\alpha},$$

$$F_J = \exp[-\beta\Lambda(\Lambda + 1)], \quad F_K = \exp(-\eta|\Delta K|) \quad (12)$$

and a standard energy gap law (see discussion above)

$$k_{fi} = (2J_f + 1) A \exp\left(-C \frac{|\Delta E|}{k_B T}\right) \quad (13)$$

for the rate constant k_{fi} of the energy transfer from a vibrational state i to an energetically lower vibrational state f , where J_f is the rotational quantum number of the final state, ΔE is the energy difference between the two states, and A and C are adjustable parameters. The significance of the correction factors F_J and F_K are discussed in part I. The rate constants for activating collisions were determined from rate constants of deactivating collisions employing detailed balance:

$$k_{if} = k_{fi} \frac{2J_i + 1}{2J_f + 1} \exp\left(-\frac{\Delta E}{k_B T}\right). \quad (14)$$

VI. EXPERIMENTAL RESULTS AND DISCUSSION

A. State-to-state cross sections for vibrational and rotational energy transfer (VV, V-T, R), order of magnitude considerations

With the described model above we have finally derived rate constants and thermally averaged cross sections for rotational and vibrational energy transfer by numerical integration of the set of differential equations and by modeling simultaneously all the kinetic traces obtained by state-resolved pump-probe spectroscopy. It should be noted that the time axis in this and all the other following cases has been converted into a reduced axis $Z_{\text{LJ}}[\text{M}]t$, which represents the number of Lennard-Jones collisions ($Z_{\text{LJ}} = 4.2 \times 10^{-10} \text{ cm}^3 \text{ s}^{-1}$, $13.4 \mu\text{s}^{-1} \text{ Torr}^{-1}$). This reduced axis with Z_{LJ} as a reference (collision number) is very convenient since all experiments at different pressures can be processed simultaneously. The program used the values calculated by the energy gap law (EGL) as a first choice, then the rates could be adjusted individually, if necessary, to account for specific small deviations from the EGL. The result of this simulation is satisfactory and shown in Fig. 4. It should be noted that the total depopulation in trace 1 in Fig. 4 mostly reflects rotational energy transfer in collisions, i.e., fast equilibration within a vibrational mode and not vibrational energy transfer which is significantly slower. Even in the case of collisional energy transfer between different (ro)vibrational states the pure rotational energy transfer plays a significant role. Although a single rovibrational state is prepared, the population is usually distributed between the manifold of rotational levels within the vibrational state before any discernible V-V transfer takes place. Therefore, true state-to-state cross sections for rovibrational energy

Model VET

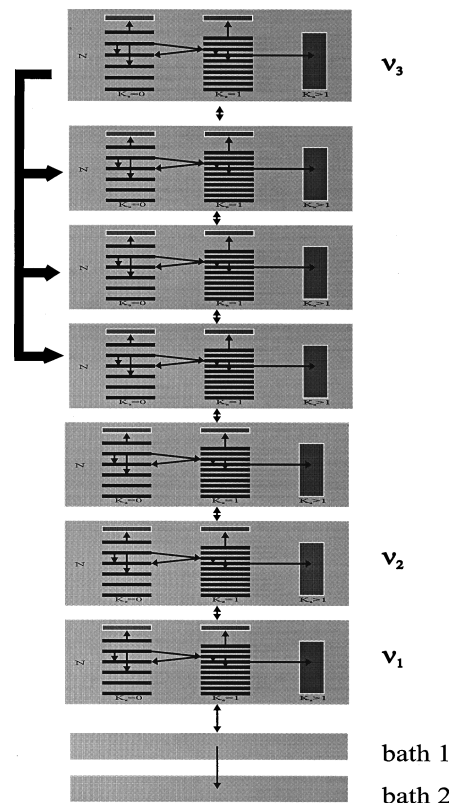


FIG. 3. Kinetic model for vibrational energy transfer between the different vibrational states in the considered energy region.

transfer can only be obtained by careful modeling of the kinetic traces. It should be pointed out that the parameters for the rotational energy transfer within a vibrational state derived in part I (m_J averaged) have been fixed and not varied, such that the good fits of rovibrational energy transfer automatically correspond to a best fit of the pure RET kinetic traces. The derived kinetic fits of state-to-state VET are depicted in Fig. 4. The state-to-state rate constants and the kinetic parameters are summarized in Fig. 5 and Tables II and III. The quoted error bars correspond to the estimated (maximum) uncertainties in the ET model and the time-resolved experimental data.

If we inspect the state-resolved cross sections for rotational and vibrational energy transfer it is obvious that the energy transfer cross sections for collisions changing the vibration and angular momentum seem to scale approximately with the energy gap ΔE between the initial and final states. As discussed above this energy gap scaling has its roots in the classical Landau-Teller and classical and modified SSH models.

If we further inspect the absolute values of the state-resolved rate constants it is striking that these are quite high with respect to the Lennard-Jones collision number. The reason for the high cross sections for rovibrational energy transfer is not clear *a priori*.

As has been shown by Barker *et al.*¹⁸ and Dai *et al.*¹⁵ the energy transfer between highly excited $\text{NO}_2^{\#}$ is dominated by V-T transfer if the collision partner is small (noble gases,

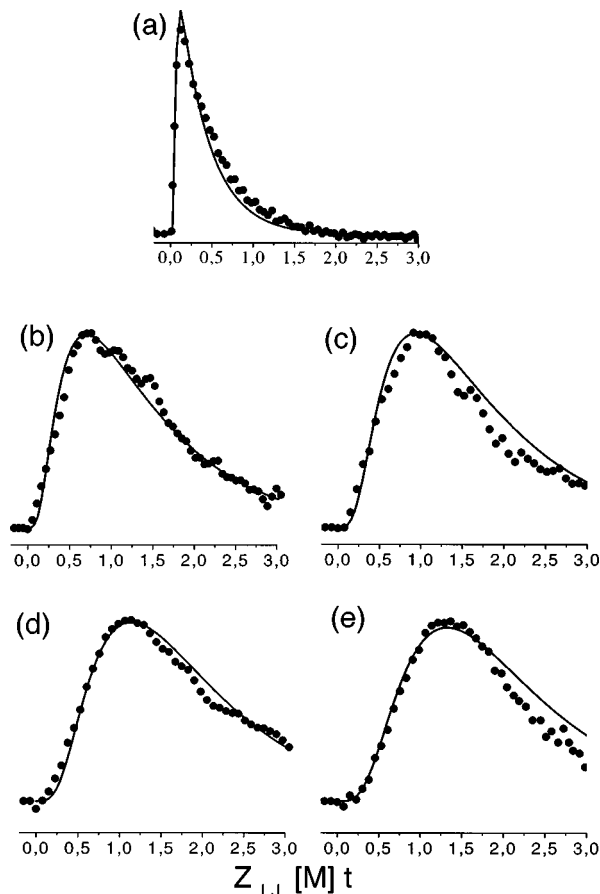


FIG. 4. Kinetic traces for rovibrational energy transfer between different rovibrational states. Filled circles: experimental traces; solid line: fit from the model. In all cases the 90(3) state has been pumped (see Table I). Probed levels: (a) 90(3), (b) 90(1), (c) 70(1), (d) 50(1), and (e) 30(1). Note: the time axis is a reduced axis here displaying the number of Lennard-Jones collisions.

diatomics, most of the triatomics). This is also the case for NO_2 self-collisions. The main energy transfer pathway for the collisions observed in this work appears to be “intramolecular $V-V$ energy transfer” according to Eqs. 2(a) and 2(b) which can be regarded as a special relaxation pathway occurring preferentially in cases of relatively small energy gaps ΔE when initial and final states are almost isoenergetic.

TABLE II. Parameters for the kinetic VRET model.

Parameters	Numerical value ^a	Dimension
Rotational energy transfer (m_j averaged): $J, K \rightarrow J', K'$		
Electron capture spectroscopy scaling		
$a(\text{T})$	$9(\pm 1) \times 10^{-10}$	$\text{cm}^3 \text{s}^{-1}$
α	$1(\pm 0.1)$	—
β	$2.4(\pm 0.3) \times 10^{-2}$	—
η	$1.5(\pm 0.2)$	—
Vibrational energy transfer: $J, K, v_i \rightarrow J', K', v_j$ with $v_i \neq v_j$		
Energy gap law scaling		
$k = k_0 \cdot \exp(-C \cdot \Delta E_{ij} /k_B T)$		
k_0	$2.5(\pm 1) \times 10^{-10}$	$\text{cm}^3 \text{s}^{-1}$
C	$23(\pm 3)$	—

^a k_{σ} ($\text{cm}^3 \text{s}^{-1}$) is given here; to obtain the cross sections σ (\AA^2), multiply by 1.912×10^{11} ; to obtain k_T ($\mu\text{s}^{-1} \text{Torr}^{-1}$), multiply by 3.2624×10^{10} .

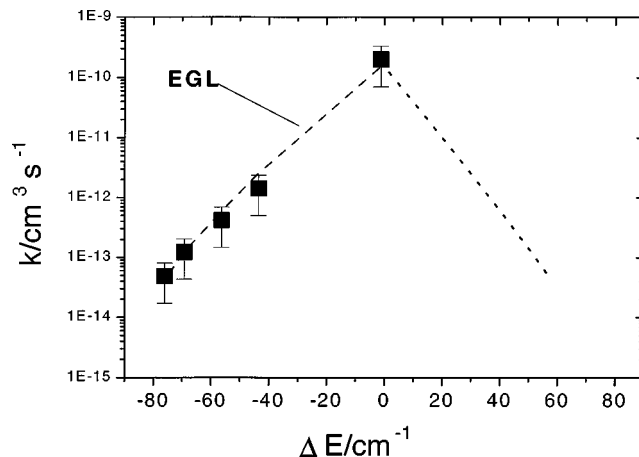


FIG. 5. Individual state-to-state rate constants as a function of ΔE for rovibrational energy transfer between different rovibrational states. In all cases the 90(3) state has been pumped (see Table I). Probed levels: 90(2), 90(3), 90(1), 70(1), 50(1), and 30(1). Long dashed line: energy gap law (EGL), see Table II and III) Short dashed line: EGL prediction for not observed “upward” transitions.

Total relaxation rates are known for the lower excited states of NO_2 (below the origin of the 2B_2) and are found to be on the order of $0.01 k_{\text{LJ}}$ with an overall linear increase with increasing internal energy.^{39–42} We found it interesting to compare total relaxation rates at high internal energies (strongly mixed states) with these low energy rates. Although, we have measured state-resolved relaxation data, these data can, in principle, be used to estimate total relaxation rates using our model, the known average density of states, as well as the scaling behavior for the individual state-to-state rate constants (summation without $R-R$ energy transfer). The determination of total relaxation rates k_{tot} from our model is quite uncertain, but nonetheless a value on the order of $k_{\text{LJ}} \approx 1-2 \times 10^{-10} \text{ cm}^3 \text{s}^{-1}$ (with quite large error bars) was estimated. This value is close to the relaxation rates measurement of Donnelly *et al.*³⁸ who measured a total relaxation rate of $1.2 \times 10^{-10} \text{ cm}^3 \text{s}^{-1}$ in NO_2 self-collisions at $E = 18\,800 \text{ cm}^{-1}$. It is interesting to note that there seems to be a large difference between relaxation rates below about $9000-10\,000 \text{ cm}^{-1}$ and above, given that the experimental rates are correct and can be compared (see Fig. 6). This could be explained by a strong energy dependence of the relaxation rates resembling the strong energy dependence of $\langle \Delta E(E) \rangle$ as a function of internal energy that has been found by Dai *et al.*^{15,52} and Barker *et al.*¹⁸ Without speculating too much one may nevertheless ask where this energy dependence comes from.

In the following, we will discuss three possible mechanisms which have been suggested and invoked to explain enhanced rovibrational energy transfer and its energy dependence in the impulsive (sudden) and/or the complex forming limit, i.e., in the case where nonadiabatic transitions in the collision complex at short or large distances play a role rather than kinematics.

- One attempt to explain these high relaxation rates (without being able to explicitly explain their conjectured energy dependence) is related to the fact that NO_2

TABLE III. Direct state-to-state rate coefficients and cross sections from the kinetic VRET model. Vibrational energy transfer: $J, K, \nu_i \rightarrow J', K', \nu_j$ with $\nu_i \neq \nu_j$.

$J, K, \nu_i \rightarrow J', K', \nu_j^a$	ΔJ	ΔK	ΔE (cm ⁻¹)	k_σ (cm ³ s ⁻¹) ^b	k_T (μ s ⁻¹ Torr ⁻¹)	σ (Å ²)	Obs. (+) pred. (0)
7,0 (1) \rightarrow 7,0 (2)	0	0	-1.9	2.1×10^{-10}	6.8	40.1	+
9,0 (3) \rightarrow 9,0 (1)	0	0	-44.1	1.5×10^{-12}	4.9×10^{-2}	0.29	+
9,0 (3) \rightarrow 7,0 (1)	-2	0	-56.6	4.4×10^{-13}	1.4×10^{-2}	8.4×10^{-2}	+
9,0 (3) \rightarrow 5,0 (1)	-4	0	-69.7	1.2×10^{-13}	3.9×10^{-3}	2.3×10^{-2}	+
9,0 (3) \rightarrow 3,0 (1)	-6	0	-76.3	5.0×10^{-14}	1.6×10^{-3}	9.6×10^{-3}	+

^aFor the coding of single states see Table I.^b k_σ (cm³ s⁻¹) multiplied by 1.912×10^{11} yields σ (Å²) and k_σ (cm³ s⁻¹) multiplied by 3.2624×10^{10} yields k_T (μ s⁻¹ Torr⁻¹).

is actually a free radical and each energy level is split into two spin components. Up to now we have treated the molecule like a closed shell molecule. This seemed to work fine as far as scaling of individual relaxation rates is concerned. However, open shell effects may be responsible for explaining the large magnitude (amplitudes) of the observed cross sections for vibrational and rotational energy transfer.⁵³

- (b) Considering the first Born approximation it is obvious that intramolecular vibrational energy transfer ($V-V$) is strongly enhanced when relatively small energy gaps exist, because such a transition can be brought about by the long-range interactions of the molecules which are correlated with quite large impact parameters and in turn with quite high cross sections.
- (c) A third explanation involves vibronic mixing of the states of the highly excited molecules. As it was shown by Orr *et al.*⁵ vibrational energy transfer between states sharing a common perturbation (or involving states that are even strongly mixed) may show strongly enhanced vibrational energy transfer compared to the unperturbed case.

We will now inspect the suggested models for the strong enhancement of vibrational energy transfer and discuss them

with respect to both order of magnitude and the energy dependence of the cross sections. In particular, we will rule out impulsive or complex forming collisions if we compare the data with reactive thermally averaged cross sections, i.e., the high pressure limiting rate constant $k_\infty(T)$ being close to 9×10^{-12} cm³ s⁻¹ (Ref. 54).

As discussed already by Nikitin,⁵³ a possible explanation for the high efficiency of the vibrational relaxation of open shell molecules involves nonadiabatic crossings. He discussed that when one or both collision partners are in a degenerate electronic state, intermolecular interactions lift the electronic degeneracy such that when molecules approach, there arises a whole set of adiabatic potential energy surfaces for each vibrational state which are strongly coupled and may cross even beyond the “collision complex” (e.g., at large intermolecular distance) which in turn can enhance $V-T$ vibrational energy transfer. This model was employed some time ago to describe the large $V-T$ cross sections found for vibrational energy transfer in NO-NO collisions.

Within the framework of extended adiabatic channel models¹² (that are able to explicitly treat nonadiabatic transitions) one explanation for the large relaxation rates ($E > 9000$ cm⁻¹) is that long-range electronically excited states of N₂O₄ [correlating with NO₂(²A₁) and NO₂(²B₂)] with no or shallow minima may nonadiabatically cross at large distances (in order to account for the large overall cross sections). In such a case a real long lived complex is not necessary but strong coupling between the two collision partners is. These nonadiabatic transitions may also be mediated by electronically excited states at large distances correlating with NO₂⁻ and NO₂⁺ (estimations of these effects from ionization energies and electron affinities make this possibility unlikely). If these crossings occur at large distances this would correspond to a large enhancement of $V-T$ energy transfer cross section mechanics, however, it is quite difficult to derive general scaling laws from theory in this case.

Unfortunately, the observed cross sections (overall and state-to-state rates) are much higher than the high pressure limiting rate constant,⁵⁴ and the energy dependence of the total relaxation rate seems to correlate with the onset of the ²B₂ electronically excited state of NO₂ rather than with properties of N₂O₄ such that energy transfer models involving nonadiabatic transitions appear to be unable to explain all our observations.

The latter theoretical models compete with the more

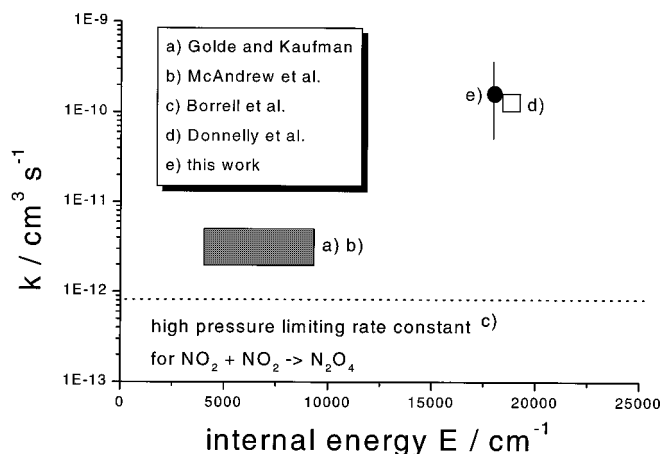


FIG. 6. Comparison of the summed state-to-state constants at $E \approx 18\,000$ cm⁻¹ from this work (rotational energy transfer within a vibration excluded) with rate constants: (a) from Golde and Kaufman, (b) McAndrew *et al.*, (c) the high pressure limiting rate constant $k_\infty(T)$ from Borrell *et al.*, and (d) the rate constants from Donnelly *et al.*

qualitative impulsive models based on Landau–Teller–SSH theory and their modifications and the Born approximation in quantum mechanics. However, even for collision mechanisms in the impulsive limit there are several possibilities to explain large and strongly increasing relaxation rates as a function of internal energy (as suggested in Fig. 6).

If we inspect the expression for the first Born approximation,

$$P_{if}(\Delta\omega) = \hbar^{-2} \left| \int_{-\infty}^{\infty} V_{if}(t) \exp(i\Delta\omega t) dt \right|^2$$

with

$$V_{if} = \langle i | V(t) | f \rangle, \quad (15)$$

it is easily shown in Eq. (15) that the probability will be maximized when $V_{if}(t)$ has Fourier components at frequency $\Delta\omega$. For a V – T process [Eq. (2)] where $\Delta\omega$ is large this may be only achieved on the repulsive part of the interaction potential where $V_{if}(t)$ changes rapidly with time. If $\Delta\omega$ is small for an intermolecular V – T process [Eq. (2)] or an intramolecular V – V process [Eq. (3)] the attractive long-range part of the interaction potential may introduce considerable Fourier components at a frequency $\Delta\omega$ into $V(t)$. With this very simple qualitative or at most semiquantitative approach, high relaxation rates can be understood in terms of strongly enhanced intramolecular vibrational energy transfer (V – V) which is a special form of vibrational energy transfer when relatively small energy gaps exist, because such a transition can be brought about by the long-range interactions of the molecules which are correlated with quite large impact parameters and in turn with quite high cross sections. The Born approximation expression also provides (a more qualitative) interpretation for the energy dependence of the relaxation rates if one takes the excited state coupling of the 2A_1 and 2B_2 states of NO_2 explicitly into account. An inspection of Eq. (15) shows again that the probability P_{ij} will be maximized when $V_{if}(t)$ has Fourier components at frequency $\Delta\omega$. For small $\Delta\omega$ the attractive long-range interaction potential may be responsible for considerable Fourier components. At the initial energy in our energy transfer experiments, the amplitude of the motion can already be quite large and irregular at an energy equal to 3/4 of the dissociation energy E_0 . The large amplitude and irregular motion may produce very low frequencies of the motion.¹⁸ Equation (15) indicates that the lower the frequency, the larger the probability P_{ij} at a given temperature and (low) collision energy. As the system energy is reduced, the large amplitude motions and the excited state mixing causing irregular behavior are reduced. Below the energy of the first excited state 2B_2 the motion is confined to the lowest potential energy surface and the states are regular, thus, the probability for V – T transfer (also intramolecular) is markedly decreased.

In the basic SSH model the probability P_{ij} for the transition $i \rightarrow j$ is proportional to the squared coupling matrix element U_{if}

$$P_{ij} \propto |U_{if}|^2. \quad (16)$$

It predicts a linear increase of the probabilities for V – T energy transfer as a function of increasing vibrational quantum

number ν . The probability for multiquanta transitions (corresponding to large energy gaps or small energy gaps in the case of collisionally induced V – V intramolecular energy transfer) is generally very low. This is clearly not sufficient to describe the experimental results. This situation changes considerably when state mixing is considered. The electronic structure of NO_2 has been investigated by many groups including our own. It is established that several electronic excited states are strongly coupled with the ground state at high energies. This is particularly true for the lowest excited 2B_2 state which has its origin between 9000 and 10 000 cm^{-1} causing even vibronic chaos above 17 000 cm^{-1} . In the following we will qualitatively explore how state mixing may affect the matrix element U_{if} in Eq. (16). Following Orr *et al.*⁵ the general situation can be illustrated by considering a transition between two eigenstates $|I\rangle$ and $|II\rangle$, which can be expressed as simple mixtures of two unperturbed states $|A\rangle$ and $|B\rangle$, that is

$$|I\rangle = C_a |A\rangle + C_b |B\rangle, \quad (17a)$$

$$|II\rangle = C_b |A\rangle - C_a |B\rangle. \quad (17b)$$

Note that this model can easily be extended to more coupled electronic and vibrational states. With the above defined wave functions the vibrational matrix element U_{if} is

$$\begin{aligned} U_{if} &= \langle \Psi_I | V(Q_1, Q_2, \dots) | \Psi_{II} \rangle \\ &= C_a C_b (\langle A | V | A \rangle - \langle B | V | B \rangle) + (C_b^2 - C_a^2) \langle A | V | B \rangle. \end{aligned} \quad (18)$$

Depending strongly on the mixing coefficients C_a and C_b , as well as the matrix elements $\langle A | V | A \rangle$, $\langle B | V | B \rangle$, and $\langle A | V | B \rangle$, U_{if} can be smaller (in a few cases⁵) or much larger than in the unperturbed case. However, their combined contributions may not be immediately obvious, since quantum interference effects can arise. This has been shown and pointed out by Orr *et al.*⁵ and Parmenter and Knight,⁵⁵ and just recently by Dai and collaborators.⁵² For the particular case of NO_2 the rovibronic wave functions of the mixing 2A_1 and 2B_2 electronic states have to be taken into account properly. In doing so Dai *et al.* showed that the analogous evaluation suggests that the off-diagonal terms in Eq. (19), which are assumed to be connected with the electronic transition dipole moment and the long-range dipole interaction, may play a big role and considerably increase U_{if} in this case. They therefore explain the strong energy dependence of the average energy transferred in a collision $\langle \Delta E \rangle$ as being possibly caused by the electronic transition dipole moment and the strong long-range dipole interaction. Whether the electronic transition dipole moment plays such an outstanding and dominant role or not has to be verified. However, we also point out that state mixing in NO_2 above the origin of the 2B_2 state may also explain the (experimental) relaxation rates.

B. Direct versus complex forming collisions, absolute rate coefficients in comparison with high pressure rate constants

As has been discussed earlier the energy transfer events can be characterized by direct or complex forming collisions

depending on the impact parameter, the intermolecular interaction, and the collision energy. However, these cases are certainly limiting cases and there is no clear prescription how to distinguish cases in between. Although there is no absolute definition of complex formation, the criterion of Schatz and Lendvay employed in their study of temporal histories of trajectories may be useful.¹⁰ Another but not very stringent and reliable criterion is the Massey parameter ξ . For values of the parameter very much smaller than 1 the collision dynamics is close to the impulsive limit. Simple estimations show that ξ for the present case of small ΔE at high internal energies is less than 1 but not very much less for larger energy gaps. We are aware of the fact that such an estimation is very crude and much less meaningful than in the case of rotational energy transfer (see part I) and, in particular, that values for the adiabatic parameter larger than 1 do not necessarily correspond to complex forming collisions! Therefore estimations based on the Massey parameter or adiabatic parameters should be considered with caution and not overinterpreted.

A better criterion to distinguish complex forming collisions from impulsive ones and any collision situation in between is to compare the cross sections with truly complex forming collisions in a thermal ensemble, namely reactive collisions. It has been shown by Quack and Troe,⁵⁶ Troe *et al.*,⁵⁷ and Smith and co-workers⁵⁸ both theoretically and experimentally that the high pressure limiting rate constant $k_{\infty}(T)$ may, under certain conditions and to a very good approximation, be equal to the total vibrational relaxation rate. Just recently Smith⁴⁴ has summarized and reviewed the state-of-the-art experiments and results that prove this hypothesis. The comparison with the high pressure rate constant (which is available from Ref. 54) is the least biased criterion to decide the mechanism of the $\text{NO}_2^{\#}\text{-NO}_2$ collisions at high internal energies, and at low internal energies. In Fig. 6 we have compared the total vibrational relaxation rate for $\text{NO}_2\text{-NO}_2$ collisions in the $18\,000\text{ cm}^{-1}$ energy region derived from our model ($\sum k_{ijvv'}$, with $v \neq v'$) with the relaxation data in the energy region below 9000 cm^{-1} from Refs. 41–42. Also indicated is the value of the limiting high pressure rate constant for the reaction $\text{NO}_2 + \text{NO}_2 \rightarrow \text{N}_2\text{O}_4$. We have already pointed out that the high energy data are quite different in magnitude than the low energy data. We have also tried to give an explanation for this in the framework of time dependent perturbation theory and impulsive models without consideration of collision complexes. Comparing the order of magnitude of the high pressure rate constant $k_{\infty}(T)$ with the state-resolved data from this work we conclude that the collisions we observe are not complex forming collisions, although we have strong attractive chemical forces present in our system. This may in part be explained by the large excess energy with respect to the dissociation energy of the $\text{N}_2\text{O}_4(4430\text{ cm}^{-1})$ which is still small compared to other chemical bond energies. Let us for a moment assume that such a collision proceeds via a collision complex where vibrational energy transfer is made by nonadiabatic transitions between excited state potential energy curves of the N_2O_4 molecules. If the potential energy surface possesses an attractive well, a long lived collision complex (N_2O_4) may be

formed. Classically, this would result from orbiting collisions such as described above. The quantum analogue is a resonance which can occur when the collision energy matches that of a bound state in the potential well or a scattering state above the dissociation threshold of the complex, in this case a bound molecule N_2O_4 . However, if we have an excitation energy of $17\,800\text{ cm}^{-1}$, i.e., more than $13\,000\text{ cm}^{-1}$ of excess energy above E_0 of N_2O_4 all resonances in the quasicontinuum with respect to the ground state potential are very broad and diffuse. They most likely do not support “orbiting” collisions nor long lived complexes, nor complete energy randomization within the complexes. If we were to invoke excited states of N_2O_4 and nonadiabatic transitions between the corresponding potential surfaces (e.g., by ion pair potentials) at long distances this model may hold. However, we have no information about and evidence of the excited electronic states nor crossings with ion pair potentials at large distances enhancing nonadiabatic transitions. However if they exist the corresponding collisions mimic and resemble collisions which are closer to the impulsive limit than the complex limit.

Comparing the high pressure rate constant with the relaxation data at low energies we find that they are much closer, although the relaxation data are still significantly higher. Taking into account all error bars for the determination of high pressure rate constants and total relaxation in the NO_2 system (which is not an easy task) we conclude that the relaxation data are consistent with the relaxation data within a factor of about 2.

We are therefore left in a situation where we have to explain why collisions at low energies appear to be (formally) closer to the complex forming limit and collisions in highly excited states appear to be formally (and the scaling behavior) consistent with more impulsive (not complex forming) collisions. A possible explanation for this behavior is that $V\text{-}V$ intramolecular energy transfer, in the limit of strong intramolecular state mixing involving small energy gaps, can be brought about very efficiently (with high cross sections) by very small perturbations at large impact parameters. This effect may even be enhanced by excited states (maybe through a large transition dipole moment). Recently, Lendvay and Schatz have (qualitatively) pointed out the role and dominance of impulsive “fast” collisions in the energy transfer of small molecules.¹⁰ They have studied the temporal history of many classical trajectories and found that only in a small fraction of collisions a complex is formed. However, these results have been obtained for systems with much less strong intermolecular interaction and the agreement between calculated and experimental $\langle \Delta E \rangle$ (average amount of energy transferred in a collision) was still not perfect. If the intramolecular state mixing becomes smaller or absent and the energy gap becomes larger the repulsive part of the potential becomes more important. $V\text{-}T$ energy transfer with large energy gaps is much less efficient such that complex forming collisions and $V\text{-}V$ energy transfer can effectively compete. Complex forming collisions between radicals in a situation where the collision energy and the excess energy (with respect to D_0) are low may play a much more important role than in the high energy limit. In this case the com-

plex forming collisions are highly competitive in transferring larger amounts of energy compared to the impulsive ones. In this case it is not surprising that the relaxation rate, which may be dominated by complex forming collisions, is close to $k_{\infty}(T)$.

VII. CONCLUSIONS

In summary, we have measured collisionally induced intramolecular $V-V$ and intermolecular $V-T$ energy transfer at chemically relevant internal energies ($3/4$ of E_0 of NO_2) employing a novel time-resolved optical-optical double resonance technique. State-resolved rovibrational energy transfer cross sections could be measured. It has been found that the state-resolved rate constants could be scaled by a simple energy gap law. The order of magnitude of the observed rates is quite large with respect to the Lennard-Jones collision frequency and the high pressure limiting rate constant, indicating that the collisions follow an impulsive mechanism rather than a complex forming mechanism. From the averaged rates, total relaxation rates have been estimated which have been compared with relaxation rates at lower energies. They seem to suggest a strong energy dependence of the total relaxation rate as a function of energy. Attempts to explain this behavior have been made within the framework of time-dependent perturbation theory. The data obtained for a small molecule at chemically significant energies strongly support our conclusion that the total (rovibrational) relaxation rate at very high internal energies is not necessarily close or equal to the high pressure limiting rate constant. We have discussed the conditions (large energy gaps and low internal and collision energies) for which relaxation rates and recombination rates at high pressure are close.

ACKNOWLEDGMENTS

We enjoyed many stimulating discussions with Klaus Luther, Jeff Steinfeld, Steve Coy and Brian Orr. Financial support from the Deutsche Forschungsgemeinschaft (SFB 357 "Molekulare Mechanismen Unimolekularer Prozesse", AB 63/2-1/2) is gratefully acknowledged. The authors thank Steve Coy for the MATLAB and FORTRAN routines for some of the $3J$ symbol calculations. F.R. thanks the "Fond der Chemischen Industrie" and the BMFT for a graduate student fellowship.

¹H. Hippler and J. Troe in *Bimolecular Collisions (Advances in Gas-Phase Photochemistry and Kinetics)*, edited by M. N. R. Ashfold and J. E. Baggott (The Royal Society of Chemistry, London, 1989).

²R. G. Gilbert and S. C. Smith, *Theory of Unimolecular and Recombination Reactions* (Blackwell Scientific, Oxford, 1990).

³J. T. Yardley, *Introduction to Molecular Energy Transfer* (Academic, New York, 1980).

⁴R. E. Weston and G. W. Flynn, *Annu. Rev. Phys. Chem.* **43**, 559 (1992).

⁵(a) B. J. Orr, *Advances in Chemical Kinetics and Dynamics*, (JAI, New York, 1995), Vol. 2A, p. 21; (b) B. J. Orr and I. W. M. Smith, *J. Phys. Chem.* **91**, 6106 (1987).

⁶G. W. Flynn and R. E. Weston, *Advances in Chemical Physics and Dynamics* (JAI, New York, 1995), Vol. 2B, p. 359.

⁷Atom-Molecule Collision Theorie: A Guide for the Experimentalist, edited by R. B. Bernstein (Plenum, New York, 1979).

⁸E. E. Nikitin and S. Ya. Umanskii, *Theory of Slow Atomic Collisions*, Springer Series in Chemical Physics, Vol. 30 (Springer, New York, 1984).

⁹D. C. Clary and G. J. Kroes, *Advances in Chemical Kinetics and Dynamics* (JAI, New York, 1995), Vol. 2A, p. 135.

¹⁰G. Lendvay and G. C. Schatz, *Advances in Chemical Physics and Dynamics* (JAI, New York, 1995), Vol. 2A, p. 481.

¹¹B. Pouilly, J.-M. Robbe, and M. H. Alexander, *J. Phys. Chem.* **88**, 140 (1984).

¹²(a) I. Koifman, E. I. Dashevskaya, E. E. Nikitin, and J. Troe, *J. Phys. Chem.* **99**, 15348 (1994); (b) E. E. Nikitin, J. Troe, and V. G. Ushakov, *ibid.* **98**, 3257 (1994).

¹³E. E. Nikitin, in *Physical Chemistry: An Advanced treatise*, edited by H. Eyring, D. Henderson, and W. Jost (Academic, New York, 1974), Vol. 6A.

¹⁴B. Abel, B. Herzog, H. Hippler, and J. Troe, *J. Chem. Phys.* **91**, 900 (1989).

¹⁵G. V. Hartland, D. Qin, and H.-L. Dai, *J. Chem. Phys.* **100**, 7832 (1994); **101**, 1 (1994); **102**, 8677 (1995).

¹⁶U. Hold, T. Lenzer, K. Luther, K. Reihs, and A. Symonds, *Ber. Bunsenges. Phys. Chem.* **101**, 552 (1997).

¹⁷B. Abel, H. Hippler, and J. Troe, *J. Chem. Phys.* **96**, 8872 (1992).

¹⁸B. M. Toselli, T. L. Walunas, and J. R. Barker, *J. Chem. Phys.* **92**, 4793 (1990).

¹⁹(a) A. P. Milce, H.-D. Barth, and B. J. Orr, *J. Chem. Phys.* **100**, 2398 (1994); (b) A. P. Milce and B. J. Orr, *ibid.* **104**, 6423 (1996).

²⁰J. D. Tobiasson, M. D. Fritz, and F. F. Crim, *J. Chem. Phys.* **101**, 9642 (1994).

²¹J. Wu, R. Huang, M. Gong, A. Saury, and E. Carrasquillo, *J. Chem. Phys.* **99**, 6474 (1993).

²²P. H. Vaccaro, F. Temps, S. Halle, R. W. Field, and J. L. Kinsey, *J. Chem. Phys.* **87**, 1895 (1987).

²³F. Temps, S. Halle, P. H. Vaccaro, R. W. Field, and J. L. Kinsey, *J. Chem. Soc., Faraday Trans. 2* **84**, 1457 (1988).

²⁴B. Abel, H. H. Hamann, and N. Lange, *Faraday Discuss.* **102**, 147 (1995).

²⁵J. J. Klaassen, S. L. Coy, J. I. Steinfeld, and B. Abel, *J. Chem. Phys.* **101**, 10533 (1994).

²⁶B. Abel, S. L. Coy, J. J. Klaassen, and J. I. Steinfeld, *J. Chem. Phys.* **96**, 8236 (1992).

²⁷R. Doppeide, W. Cronrath, and H. Zacharias, *J. Chem. Phys.* **101**, 5804 (1994).

²⁸K. Takayanagi, *J. Phys. Soc. Jpn.* **45**, 976 (1978).

²⁹K. Sakimoto, *J. Phys. Soc. Jpn.* **48**, 1683 (1980).

³⁰E. I. Dashevskaya, E. E. Nikitin, and J. Troe, *J. Chem. Phys.* **97**, 3318 (1992).

³¹R. N. Schwartz, Z. I. Slawsky, and K. F. Herzfeld, *J. Chem. Phys.* **20**, 1591 (1952).

³²F. I. Tanczos, *J. Chem. Phys.* **25**, 439 (1956).

³³J. L. Stretton, *Trans. Faraday Soc.* **61**, 1053 (1965).

³⁴C. S. Parmenter and K. Y. Tang, *Chem. Phys.* **27**, 127 (1978).

³⁵S. H. Kable, J. W. Thoman, and A. E. W. Knight (private communication).

³⁶R. E. Smalley, L. Warton, and D. H. Levy, *J. Chem. Phys.* **63**, 4977 (1975).

³⁷J. L. Hardwick, *J. Mol. Spectrosc.* **109**, 85 (1985).

³⁸V. M. Donnelly, D. G. Keil, and F. J. Kaufman, *J. Chem. Phys.* **71**, 659 (1979).

³⁹(a) S. M. Alder-Golden, *J. Phys. Chem.* **93**, 691 (1989); (b) **93**, 684 (1989).

⁴⁰J. Troe, *Ber. Bunsenges. Phys. Chem.* **39**, 144 (1969).

⁴¹T. L. Mazely, R. R. Friedl, and S. P. Sander, *J. Chem. Phys.* **100**, 8040 (1994).

⁴²J. J. F. McAndrew, J. M. Preses, R. E. Weston, and G. W. Flynn, *J. Chem. Phys.* **90**, 4772 (1989).

⁴³C. Bieler and H. Reisler, *J. Phys. Chem.* **100**, 3882 (1996).

⁴⁴I. W. M. Smith, *J. Chem. Soc., Faraday Trans.* **93**, 3741 (1997).

⁴⁵(a) B. Abel, N. Lange, F. Reiche, and J. Troe, *J. Chem. Phys.* **110**, 1389 (1999), preceding paper; (b) K. Aoki, H. Nagai, K. Hoshina, and K. Shibuya, *J. Phys. Chem.* **97**, 8889 (1993).

⁴⁶K. E. Hallin and A. J. Merer, *Can. J. Phys.* **54**, 1157 (1976).

⁴⁷W. C. Bowman and F. C. De Lucia, *J. Chem. Phys.* **77**, 92 (1982).

⁴⁸A. Delon, R. Jost, and M. Lombardi, *J. Chem. Phys.* **95**, 5701 (1991).

⁴⁹D. K. Hsu, D. L. Monts, and R. N. Zare, *Spectral Atlas of Nitrogen Dioxide 553 to 648 nm* (Academic, New York, 1978).

⁵⁰R. Georges, A. Delon, and R. Jost, *J. Chem. Phys.* **103**, 1732 (1995).

- ⁵¹J. T. Yardley and C. B. Moore, J. Chem. Phys. **46**, 4491 (1967).
⁵²G. V. Hartland, D. Qin, H.-L. Dai, and C. Chen, J. Chem. Phys. **107**, 2890 (1997).
⁵³E. E. Nikitin, Opt. Spectrosc. **9**, 8 (1960).
⁵⁴P. Borrell, C. J. Cobos, and K. Luther, J. Phys. Chem. **92**, 4377 (1988).
⁵⁵A. E. W. Knight and C. S. Parmenter, J. Phys. Chem. **87**, 417 (1983).
⁵⁶M. Quack and J. Troe, Ber. Bunsenges. Phys. Chem. **79**, 170 (1975).
⁵⁷D. Fulle, H. F. Hamann, H. Hippler, and J. Troe, J. Chem. Phys. **105**, 983 (1996).
⁵⁸R. P. Fernando and I. W. M. Smith, Chem. Phys. Lett. **66**, 218 (1979).